

2 (mix)

NTS HC \$4.50

X-671-73-13

PREPRINT

NASA TM X-66163

# ULTRAVIOLET PHOTOMETRY FROM THE ORBITING ASTRONOMICAL OBSERVATORY. VIII. THE BLUE Ap STARS

DAVID S. LECKRONE

(NASA-TM-X-66163)	ULTRAVIOLET PHOTOMETRY	N73-16826
FROM THE ORBITING ASTRONOMICAL		
OBSERVATORY. 8: THE BLUE Ap STARS		
(NASA) 49 p HC \$4.50	CSCL 03A	Unclas 53586
		G3/30

JANUARY 1973



**GODDARD SPACE FLIGHT CENTER**  
**GREENBELT, MARYLAND**

ULTRAVIOLET PHOTOMETRY FROM THE ORBITING ASTRONOMICAL  
OBSERVATORY. VIII. THE BLUE Ap STARS

by

David S. Leckrone

National Aeronautics and Space Administration  
Goddard Space Flight Center  
Greenbelt, Maryland

Received: \_\_\_\_\_

## ABSTRACT

The filter photometers in the Wisconsin Experiment Package on OAO-2 have been used to obtain data for a carefully selected set of 24 blue ( $B-V < 0.00$ ) Ap stars and 31 comparison standard B and A dwarfs and giants for a program of relative photometry. Observations were made in seven bandpasses over the effective wavelength range  $1430\text{\AA}-4250\text{\AA}$ . The Ap stars observed include members of the Si, Hg-Mn and Sr-Cr-Eu peculiarity classes. Most of them are too blue in B-V for their published MK spectral classes. The commonly held view that the blue Ap stars are essentially normal main-sequence B stars, consistent with their UBV colors, and that their MK classes are the spurious result of an atmospheric deficiency of helium is not supported by the ultraviolet data. The blue Ap stars are markedly deficient in emitted ultraviolet flux and are underluminous as compared to normal stars with the same UBV colors. The Hg-Mn stars appear less flux deficient in the ultraviolet for their UBV colors than do Si or Sr-Cr-Eu stars. Most of the Ap stars observed possess ultraviolet flux distributions, or ultraviolet color temperatures, consistent with their published MK spectral classes to well within the classification uncertainties. Each of them is notably inconsistent in its ultraviolet flux distribution with normal stars of similar UBV colors. This result is confirmed by ultraviolet spectrophotometry at  $10\text{\AA}$  and  $20\text{\AA}$  resolution of the Si star  $\theta$  Aur, data also obtained with OAO-2. Interesting differences in detail between  $\theta$  Aur and normal stars are evident in the latter data.

## I. INTRODUCTION

It has long been known that many of the peculiar A and B stars (hereinafter designated "Ap stars") are too blue for their spectral types (Deutsch 1947). This is particularly true for the silicon stars, some of which are as blue as  $(B-V) = -0.19$ , while being classified as late as B9 or A0 on the MK system. Deutsch (1947) suggested that such stars possess the gross characteristics of normal main-sequence B stars of similar color and that their late B-early A spectral types result from the suppression of the He I lines, which serve as spectral class indicators, by some unknown mechanism. This inference has received extensive support over the past decade. For example, studies by Searle and Sargent (1964), Mihalas and Henshaw (1966) and Jugaku and Sargent (1968) indicate that the blue ( $B-V < 0.00$ ) Ap stars possess Balmer line strengths, Balmer discontinuities and Si III/Si II line strength ratios which are consistent with their UBV colors. In addition, blue Ap stars belonging to galactic clusters occupy positions normal for their UBV colors in the cluster color-magnitude diagrams (Hyland 1967). Evidence of this sort has led to almost universal acceptance of the viewpoint that a blue Ap star possesses the mass, luminosity and atmospheric structure at depth of a normal, main-sequence B star with the same UBV colors and that any discordance between its colors and its MK spectral type is the accidental result of an atmospheric deficiency of helium (Sargent and

Searle 1967). Important corollaries to this conclusion are that the strong Ap star magnetic fields do not affect in any observable way the structure of their deeper atmospheric layers and that abnormal elemental abundances derived from weak spectral lines, observed at visible wavelengths, reflect real photospheric abundance anomalies rather than a peculiar temperature - pressure distribution.

The B stars emit a substantial fraction of their flux at wavelengths shorter than  $3000\text{\AA}$ . The general view of the blue Ap stars outlined above must therefore be regarded as incomplete until their ultraviolet flux distributions have been taken into account. That Ap star phenomena observed in the visible may be fundamentally related to phenomena observable in the ultraviolet has been amply demonstrated in several recent studies. Peterson (1970) and Wolff and Wolff (1971) suggest that variable continuous or line opacity sources at ultraviolet wavelengths may drive the photometric variability observed in the visible. The pioneering study of  $\alpha^2\text{CVn}$  from OAO-2 by Molnar (1973) strongly supports this idea. Strom and Strom (1969) have emphasized that a star of high silicon abundance may imitate in its UBV colors and Balmer discontinuity a normal star of hotter effective temperature, due to enhanced ultraviolet Si I continuous absorption. Although they undoubtedly overestimated the relative importance of Si I by ignoring other potentially important opacity sources (Peterson 1970), including the

wing of the HI  $\text{L}\alpha$  line (Klinglesmith 1972), the central idea developed by Strom and Strom merits further investigation. Using OAO-2 data, Code (1969) noted that the Si star  $\theta$  Aur is flux deficient at  $1700\text{\AA}$  for its B-V color, as compared to normal stars. Similarly in their study of "He-weak" stars Bernacca and Molnar (1972) found three probable Ap stars which appear flux deficient at  $1910\text{\AA}$  and  $2460\text{\AA}$ , even when the rather large uncertainties in their analysis are taken into account.

The present study represents the first comprehensive ultraviolet photometric survey of the blue Ap stars. Its principal aim is to determine whether the close similarity discussed above between the blue Ap stars and normal B stars with similar UBV colors is maintained at wavelengths shortward of  $3000\text{\AA}$ . Data are presented for 24 Ap stars and 31 normal comparison standard dwarfs and giants, observed with the Wisconsin Experiment Package (WEP) on OAO-2 (Code et al. 1970). Both normal and peculiar stars were chosen, with a few exceptions, for their minimal interstellar reddening and for the absence of known bright companions. Emphasis has been placed on the reduction of all the data to a self-consistent photometric system. The stars observed and the photometric observations are described in §§ II and III, respectively. The photometric comparison between Ap stars and normal stars is outlined in § IV. Intermediate band ultraviolet spectrophotometry of  $\theta$  Aur is described in § V, while § VI presents a discussion of the results obtained.

## II. THE STARS OBSERVED

Table 1 summarizes pertinent data for the Ap stars observed, while data for the normal comparison standards are given in Table 2. In most cases spectral peculiarities adopted in Table 1 represent a consolidation of peculiarity classes assigned by Osawa (1965) and by Cowley et al. (1969). Differences between these two sources are typically minor. Most of the Ap stars and most of the normal late B and early A stars considered here have been classified in a consistent way on the MK system by Cowley et al. (1969). Their classifications have been adopted wherever possible in Tables 2 and 5. Similarly, for the sake of consistency, the UBV colors of Johnson et al. (1966) were adopted wherever possible. Unfortunately, the latter source provides colors for only one third of the Ap stars of interest and had to be supplemented by data from Stepien (1968b) and from Eggen (1967).

Except for HD 184905, all of the stars observed possess color excess  $E(B-V) \leq 0.03$  relative to the Johnson (1963) standard main-sequence. A large majority of them have  $E(B-V) \leq 0.02$ . In dealing with color excesses this small, it is difficult to separate the effects of genuine interstellar reddening from the uncertainties in the UBV data or from possible small intrinsic differences between the (U-B) vs. (B-V) relations

for normal and Ap stars. In the present study stars with  $E(B-V) \leq 0.02$ , including all the Ap stars except HD 184905, were assumed to be totally unreddened. Data for normal stars with  $E(B-V) = 0.03$  were corrected for reddening, by use of the "average" extinction curve of Bless and Savage (1972), only if that correction brought their ultraviolet flux distributions into closer agreement with those of other stars of the same spectral type, possessing smaller color excesses. This rather arbitrary procedure resulted in small reddening corrections being adopted for HR 2154 and  $\delta$  Per. If any of the stars assumed to be unreddened here were in fact reddened by  $E(B-V) = 0.02$ , its normalized flux distribution, derived as discussed in § III, would be in error by about 0.07 mag, near  $1900\text{\AA}$ . It must be emphasized that such uncertainties are small compared to the intrinsic differences among stars discussed in subsequent sections.

Nearly half of the stars listed in Tables 1 and 2 are binaries. However, visual binaries with magnitude differences  $\Delta V < 2.5$  and double-lined spectroscopic binaries, with two exceptions, have been excluded. No attempt has been made to correct either UBV colors or ultraviolet apparent magnitudes of a given star for the possible presence of faint companions, such procedures being strongly subject to error. The normalized absolute flux scale discussed in § III is defined relative to unity flux at  $3320\text{\AA}$ . A faint companion which

contributes a few hundredths of a magnitude to the apparent brightness at  $3320\text{\AA}$  and which makes no measurable contribution below  $2000\text{\AA}$  will cause measured brightnesses below  $2000\text{\AA}$  to appear relatively too faint by a few hundredths of a magnitude. Because stars with known bright companions have been avoided, such distortions of the normalized flux distributions hopefully have been minimized.

The Hg-Mn stars HR 4072 and 46 Dra are of sufficient interest to be included here even though both are double-lined spectroscopic binaries. According to Conti (1970) both components of 46 Dra are Hg or Hg-Mn stars and they are similar in mass and effective temperature. Thus, the data given below for 46 Dra represent the composite of two very similar stars and a correction of UBV colors or ultraviolet flux distributions is unnecessary. A  $\Delta V = 1.7$  mag difference exists between the components of HR 4072, the brighter of which is also a Hg-Mn star (Conti 1970). The fainter companion may depress the apparent normalized flux distribution of HR 4072 by as much as 0.10 - 0.15 mag in the far ultraviolet, while causing the composite U-V color to be about 0.07 mag larger than that of the bright component alone. The simultaneous correction of the ultraviolet data and the UBV colors of HR 4072 produces no qualitative change in the results for Hg-Mn stars reported below.

### III. THE PHOTOMETRY

At this writing the OAO-2 spacecraft and the Wisconsin Experiment Package have functioned about four times longer than originally expected. Most of the observations reported here were carried out well after the nominal experiment lifetime had been exceeded. Fortunately, the long-term variations in photometer response are relatively smooth and well defined.

The present observations were obtained with the seven broad-band filters listed in Table 3, the most reliable WEP filters. An apparent stellar magnitude at effective wavelength  $\lambda$  and at a given epoch of observation is defined by

$$m(\lambda) = - 2.5 \log \left( \frac{s+\delta s-d}{c-d} - \frac{b-d}{c-d} \right)_{\lambda}. \quad (1)$$

Here  $s$ ,  $b$ ,  $c$  and  $d$  are digital counts in a given exposure time obtained for the star, the sky background, the on-board calibration source and the photometer dark current, respectively. The correction for pulse counter non-linearity,  $\delta s$ , has been derived from plots of digital counts versus analogue voltage and has proven to be independent of the epoch of observation. This non-linearity correction is important for stars brighter than  $B \approx 4.5$  but then typically only for the  $4250\text{\AA}$  bandpass. Only for the very brightest stars observed does it become significant at other wavelengths.

Non-linearity corrections are uncertain by about  $\pm 0.03$  mag.

To account for variations in  $m(\lambda)$  with time, due primarily to filter degradation and to the radioactive decay of the calibration source, one determines a correction term  $\delta m(\lambda)$  which reduces  $m(\lambda)$  to the system defined by the sensitivity of the photometers at orbit 8000. Hereinafter the discussion will deal with apparent magnitudes reduced to orbit 8000, given by

$$m'(\lambda) = m(\lambda) - \delta m(\lambda). \quad (2)$$

The  $\delta m(\lambda)$  corrections have been determined for each filter as a function of time and stellar spectral class by following variations in the data for 32 B3 to A3 dwarfs and giants, each of which has been observed at least twice during the life of the spacecraft. Many of the normal stars listed in Table 2 are included in this group. The  $\delta m(\lambda)$  corrections for filters at  $4250\text{\AA}$ ,  $3320\text{\AA}$ ,  $2980\text{\AA}$  and  $2460\text{\AA}$  are typically less than 0.1 mag, with an uncertainty of  $\pm 0.01$  mag, and are independent of spectral class over the range B3-A3. The  $1910\text{\AA}$  filter has degraded by nearly 0.5 mag since orbit 10,000 but its degradation is smooth and well defined to within  $\pm 0.01$  mag and is independent of spectral class over the interval B3-A3. The bandpasses at  $1550\text{\AA}$  and  $1430\text{\AA}$  have diminished in sensitivity by as much as 2 mag since orbit 9000. The  $\delta m(\lambda)$  corrections for the  $1550\text{\AA}$  filter are a weak function of spectral class, while those at  $1430\text{\AA}$  depend strongly on spectral class.

In the reduction of 1550Å and 1430Å data for a blue Ap star,  $\delta_m(\lambda)$  corrections appropriate to the stars' UBV colors were first applied. The star was then re-classified on the basis of its overall ultraviolet flux distribution, as discussed in §IV, and where necessary new  $\delta_m(\lambda)$  corrections were applied, consistent with that classification. The basic validity of this approach is an assumption of the present study.

Situations where the procedure led to an ambiguous choice of  $\delta_m(\lambda)$  are reflected by large uncertainties in the data given in Table 4 below. The uncertainties in the 1550Å and 1430Å data, though often large by ground-based standards, are small compared to the intrinsic differences among stars discussed in later sections and in no case are such uncertainties large enough to alter qualitative results obtained here. Full details about properties of the WEP photometers discussed above may be obtained directly from the author.

The scatter of individual observations about the mean  $\delta_m(\lambda)$  versus time relations, provides a good estimate of the random errors in the data. On the average  $m'(\lambda)$  values derived for all bandpasses from 4250Å to 1910Å were repeatable to about 0.02 mag ( $2\sigma$ ), values at 1550Å were repeatable to about 0.03 mag and those at 1430Å to about 0.04 mag.

In sections that follow normal and blue Ap stars are compared on the basis of their ultraviolet normalized absolute fluxes defined by

$$-2.5 \log F(\lambda) = m'(\lambda) - m'(3320\text{Å}) - 2.5 \log \Delta. \quad (3)$$

Values of  $-2.5 \log \Delta$ , the preliminary relative absolute calibration factors derived by Code (1971), are given in Table 3. Table 4 lists values of  $m'(\lambda)$ , the uncertainties in  $m'(\lambda)$  and values of  $-2.5 \log F(\lambda)$  for 55 normal and Ap stars. The uncertainties in  $m'(\lambda)$  reflect random errors as well as uncertainties in the  $\delta m(\lambda)$  and  $\delta s$  corrections.

The effective wavelengths utilized here are valid for a constant energy source. Model atmosphere calculations by Klinglesmith (1971) indicate that these effective wavelengths differ from those pertinent to early-type stars by no more than  $\pm 50\text{\AA}$  over the interval  $4250\text{\AA} - 1550\text{\AA}$  and by no more than  $\pm 80\text{\AA}$  at  $1430\text{\AA}$ . In the absence of detailed effective wavelength corrections and because of the preliminary nature of the absolute calibration, great caution should be exercised in comparing the values of  $-2.5 \log F(\lambda)$  given Table 4 to model atmospheres, for example. However, the data are entirely suitable for the program of gross relative photometry discussed in the sections that follow.

#### IV. COMPARISON BETWEEN NORMAL AND Ap STARS

Normalized absolute fluxes in magnitude units,  $-2.5 \log F(\lambda)$ , at each of four effective wavelengths,  $2460\text{\AA}$ ,  $1910\text{\AA}$ ,  $1550\text{\AA}$ , and  $1430\text{\AA}$ , are plotted versus U-V for normal stars and for the various classes of Ap stars in Figures 1 and 2. These plots are in effect color-color diagrams. The data for normal stars define a relatively smooth and narrow band in each diagram. The scatter in the normal star data is entirely consistent with the photometric uncertainties, residual interstellar reddening and possible minor intrinsic differences among stars of similar U-V color.

Two important properties of the blue Ap stars become apparent in Figures 1 and 2. First of all, the Ap stars are markedly fainter in  $-2.5 \log F(\lambda)$  at each effective wavelength than normal stars of similar U-V color. This result does not depend upon the choice of normalization point at  $3320\text{\AA}$ . Normalization to  $V = 0.00$  results in relative flux deficiencies for the Ap stars at least as large as those evident in Figures 1 and 2. Since the Ap stars possess absolute visual magnitudes comparable to those of normal main-sequence stars of similar UBV colors (Eggen 1967, Hyland 1967), their relative faintness in the ultraviolet implies that they are underluminous for their colors. Further, because the values of  $-2.5 \log F(\lambda)$  are independent of the radii and distances of the stars in question, it follows from these data

that  $(f_{\lambda}/f_V)_p < (f_{\lambda}/f_V)_n$ . Here,  $f_{\lambda}$  and  $f_V$  denote absolute fluxes emitted by unit surface area at the star, at effective wavelength  $\lambda < 3320\text{\AA}$  and at the effective wavelength of the V band, respectively. Subscripts p and n refer to a blue Ap star and a normal star, respectively, with the same intrinsic UBV colors or equivalently (Jugaku and Sargent 1968) with the same Balmer discontinuity and Paschen slope. Clearly,  $(f_{\lambda})_p < (f_{\lambda})_n$  if  $(f_V)_p \lesssim (f_V)_n$ . This condition certainly holds for  $\alpha^2\text{CVn}$  (Molnar 1972) and for the galactic cluster Si stars observed by Hyland (1967), contingent only on the assumption that the Ap stars possess radii not significantly smaller than normal for their UBV colors and absolute visual magnitudes. The latter assumption is strongly supported by the Ap star period-line width relation (Preston 1970). Moreover, ultraviolet line-blanketed and unblanketed model atmospheres which predict identical Balmer discontinuities and Paschen slopes also predict equal values of  $f_V$  to better than 1 percent, even though their ultraviolet flux distributions and effective temperatures differ significantly (e.g., Adams and Morton 1968). Thus, it appears reasonable to assume that  $(f_V)_p \lesssim (f_V)_n$  and it follows that the blue Ap stars emit less ultraviolet flux and are cooler in effective temperature than normal stars with similar UBV colors.

Secondly, the Hg-Mn stars are clearly distinguishable in Figures 1 and 2 from other classes of Ap stars. As compared

to normal stars, the Hg-Mn stars are less flux deficient in the ultraviolet, for their UBV colors, than are the Si or Sr-Cr-Eu stars. The weight of evidence from ground-based observations now supports the view that the Hg-Mn stars are innately different from other Ap stars (Preston 1971). They show no periodic variability, they have weak or non-existent magnetic fields, they exhibit a high incidence of binary membership and they possess smaller color-spectral class discrepancies than do other blue Ap stars. To this accumulated evidence may now be added the fact that they are systematically brighter in the ultraviolet than other Ap stars with similar UBV colors.

Results of particular interest are obtained when one compares the gross ultraviolet flux distribution of an individual Ap star, defined by its  $-2.5 \log F(\lambda)$  values at wavelengths  $\leq 3320\text{\AA}$ , with comparable flux distributions of normal dwarfs and giants. To establish a basis for this discussion, it must be pointed out that the ultraviolet flux distributions of normal stars, or their ultraviolet color temperatures, vary as a relatively smooth and continuous function of MK spectral class. This may readily be confirmed by use of the data given in Table 4. It is fair to say that one can estimate the MK spectral class of a normal dwarf or giant from its ultraviolet flux distribution about as well as he can on the basis of its UBV colors. Ambiguities of about 0.1 spectral classes exist over the intervals B5-B9 and A0-A2. Ambiguities of 0.05 classes appear in the range B9-A0. In the latter case, for convenience, stars whose ultraviolet flux distributions resemble

those of 134 Tau or  $\epsilon$  Hyi will be classified here as B9 (range of uncertainty B8-B9.5), those resembling  $\nu$  Cap or  $\lambda$  Cnc will be called B9.5 (range of uncertainty B9-B9.5) and those resembling  $\delta$  Cyg or  $\alpha$  Dra will be called B9.5-A0. Stars classified here as A0 have a range of uncertainty A0-A1, while those classified as A1 are uncertain within the limits A1-A2.

Figures 3, 4, 5 and 6 illustrate the detailed comparison of gross ultraviolet flux distributions of eight blue Ap stars to those of normal stars. The results of similar analyses for all 24 Ap stars treated here are summarized in Table 5. Two types of normal comparison stars are shown for each Ap star--normal stars possessing U-B or B-V colors similar to those of the Ap star and normal stars whose ultraviolet flux distributions most closely match that of the Ap star. For the sake of clarity, only a few comparison stars are illustrated in each case. The substitution of data for other normal stars listed in Table 4 does not alter the results obtained. An "ultraviolet class", defined as the MK class of the comparison stars whose ultraviolet flux distributions most closely match that of the Ap star in question, has been assigned to each Ap star in Table 5. As a specific example, although 108 Aqr (Figure 3a) possesses the same B-V as  $\delta$  For (B5) and the same U-B as  $\pi$  Cet (B7), its ultraviolet color temperature is clearly cooler than that of either of these normal stars. In fact, in the ultraviolet it very closely resembles the B9.5 star  $\lambda$  Cnc. 108 Aqr has been classified B9p, with an uncertainty

of 0.05-0.10 classes, by Cowley et al. (1969). The discussion of the other Ap stars treated here follows similar lines.

All but one of the blue Ap stars listed in Table 5 possess ultraviolet classes falling within the range B8-A2, the same range covered by their MK types. The lone exception, HD 149822, is clearly anomalous in its ultraviolet flux distribution as compared to other Ap stars of similar UBV colors and peculiarity class and will be excluded from further consideration here. The degree to which this group characteristic translates into an agreement between the MK and ultraviolet classes of individual Ap stars depends to some extent upon the source of the MK classes one adopts. Certainly, such agreement obtains for the vast majority of Ap stars considered regardless of the source of their assigned MK classes. For example, Table 5 lists classifications by Cowley et al. (1969) for 19 Ap stars, excluding HD 149822, and of these 15 possess ultraviolet classes which agree with their assigned MK types to well within the classification uncertainties, that is typically to better than 0.1 spectral classes. The four exceptions, 137 Tau, 15 Cnc (Figure 6a), 84 UMa and HD 133029, possess ultraviolet classes later than their assigned MK types by 0.1-0.3 classes. It is interesting to note that all four of these stars occupy positions in the color-color diagrams of Figures 1 and 2 consistent with other Ap stars of similar UBV colors and peculiarity classes. Thus, the disagreement between their MK and ultraviolet classes does not reflect anomalously cool ultraviolet color temperatures but rather, anomalously early MK classes as compared to other Ap stars. Indeed, if their B9p classes are valid, these four

stars would seem not to possess significant UBV color-spectral type discrepancies, unlike most other blue Ap stars. Agreement between ultraviolet and MK classes is substantially improved for at least three of these stars if one adopts MK classes derived by other authors. Bertaud (1959) calls 84 Uma an A2 star. Babcock (1958) and Bertaud (1959) classify 15 Cnc and HD 133029 as A0. Osawa (1959) agrees with Cowley et al. (1969) in classifying 137 Tau as B9, but this class is only in marginal disagreement with its A0 ultraviolet class. Had Bertaud's (1959) compilation been adopted here as the primary source of MK types, close agreement between ultraviolet and MK classes would have been obtained for 17 of 18 stars classified.

Most of the Ap stars listed in Table 5 are too blue in B-V for their MK spectral types, as discussed in § I. Color-spectral type discrepancies as large as 0.6 spectral classes are represented. A noteworthy result of the present study is that no such color-spectral type discrepancies are evident at wavelengths shortward of 3320<sup>0</sup>Å. Ap stars with large UBV color-MK spectral type discrepancies invariably resemble normal stars of like MK class in the ultraviolet.

## V. ULTRAVIOLET SPECTROPHOTOMETRY OF $\theta$ AUR

The observational results discussed in § IV are based entirely upon broad-band filter photometry. Such photometry, though useful in delineating general trends, is not an adequate substitute for higher resolution ultraviolet spectrophotometry of the stars in question. There is cause for concern, for example, that the apparent ultraviolet flux deficiencies of the blue Ap stars in the broad-band data may merely reflect the presence of a few very strong absorption lines, lying near the center of each bandpass, and may not accurately characterize the overall ultraviolet flux envelopes of these stars.

Fortunately, a few of the Ap stars listed in Table 1 are sufficiently bright to be observable with the WEP spectrometers (Code et al. 1970). The silicon star  $\theta$  Aur has been reasonably well observed both with Spectrometer 1 (Sp 1) at about  $20\text{\AA}$  resolution and with Spectrometer 2 (Sp 2) at about  $10\text{\AA}$  resolution. Data for  $\theta$  Aur and for some normal comparison stars are illustrated in Figures 7 and 8. Also shown are the nominal half-power bandwidths of several WEP broad-band filters. The spectrometer data have been reduced only to the degree necessary for simple relative photometry. Apparent count rates were corrected for dark background, placed in magnitude units and normalized to zero magnitudes at  $3320\text{\AA}$ , in the case of Sp 1, or to  $U = 0.00$  in the case of Sp 2.

Spectrometer data of this sort are not available for all of the normal comparison stars observed with the broad-band

filters. Among the normal stars represented in the Sp 1 data collection,  $\epsilon$  And is the closest to  $\theta$  Aur in its UBV colors. From the broad-band data of Figure 1, one would expect  $\epsilon$  And to be relatively brighter than a normal star with U-V identical to that of  $\theta$  Aur by less than 0.1 mag at 1910 $\text{\AA}$  and 2460 $\text{\AA}$ . Similarly, in the broad-band data  $\beta$  CMi is only 0.02 mag brighter at 1550 $\text{\AA}$ , relative to 3320 $\text{\AA}$ , than 134 Tau, the UBV comparison standard used for  $\theta$  Aur in Figure 3b. On this basis,  $\epsilon$  And and  $\beta$  CMi adequately approximate normal stars with UBV colors like those of  $\theta$  Aur over the wavelength ranges relevant to Figures 7 and 8, respectively.

The Sp 1 and Sp 2 data generally confirm at higher resolution the trends noted in the broad-band data plotted in Figure 3b. Note, for example, that data for  $\theta$  Aur in the vicinity of 1500-1600 $\text{\AA}$  are bracketed by comparable data for the early A stars  $\gamma$  UMa and  $\gamma$  Gem both in Figure 3b and in Figure 8. At no point over the wavelength range 1500 $\text{\AA}$ -3000 $\text{\AA}$  does  $\theta$  Aur approach in relative brightness normal stars of similar UBV colors.

Interesting differences in the point-by-point structure of the spectrometer scans between  $\theta$  Aur and the normal early A-type stars are evident in Figures 7 and 8. Some absorption features appear to be enhanced in  $\theta$  Aur between 2300 $\text{\AA}$  and 3000 $\text{\AA}$  and also at 1720 $\text{\AA}$ . Enhanced line opacity from the third and fourth spectra of the rare earths may be responsible for some of the strong absorption features seen in the 2300-3000 $\text{\AA}$  interval (Dieke et al. 1961, Wolff and Wolff 1971), although

$\theta$  Aur is not reported in the literature to be a strong rare earth star in the sense of  $\alpha^2$  CVn, for example. Underhill et al. (1972) have shown that the as yet unidentified feature at  $1720\text{\AA}$  is a good indicator of stars with extended atmospheres. It is present in great strength in spectra of early-type supergiants and shell stars but is weak or absent in the spectra of dwarfs and giants. It is noteworthy that the  $1720\text{\AA}$  feature is as strong in the spectrum of  $\theta$  Aur as it is in supergiant or shell-star spectra. The feature which is commonly assumed to be the Mg II  $2800\text{\AA}$  resonance doublet in Sp 1 scans of normal stars does not appear in the scan of  $\theta$  Aur shown in Figure 7, or at least it is too weak to be resolved here, although it is evident in the comparison star scans illustrated. Finally, there is no compelling evidence in the scan of  $\theta$  Aur shown in Figure 8 for the presence of the Si I ionization edges at  $1520\text{\AA}$  and  $1680\text{\AA}$  with strengths greater than their strengths in normal stars. The weak (about 0.1 mag)  $1680\text{\AA}$  edge identified by Molnar (1973) in  $\alpha^2$  CVn may be present also in  $\theta$  Aur and in the normal stars illustrated here, but this is difficult to determine with certainty. The wavelength region near  $1680\text{\AA}$  is complicated by the apparent presence of absorption lines both in  $\theta$  Aur and in normal stars. Also, low weight must be given to the  $\theta$  Aur data point at  $1683\text{\AA}$ , there being substantial scatter at this single point between the two Sp 2 scans averaged for illustration in Figure 8.

## VI. DISCUSSION

It is now clear that the close similarity, deduced from ground-based observations, between the blue Ap stars and normal B stars is not maintained in the ultraviolet. The blue Ap stars emit less ultraviolet flux than normal stars of like UBV colors. They are underluminous and cool in effective temperature for their colors (see, e.g., Molnar 1973). Moreover, it appears from the empirical evidence that the MK spectral class of a blue Ap star is a physically meaningful parameter in the sense that, in most cases, it accurately describes the emergent flux distribution of the star in the ultraviolet. It seems unlikely that this could be the case, if the late B-early A MK class were the accidental result of an atmospheric deficiency of helium. The possibility must be reconsidered that a blue Ap star possesses an atmospheric temperature-pressure-radiation structure which differs from that of a normal B star and which may profoundly influence its observed spectrum.

Two obvious, but by no means simple, approaches to the problem might be taken. The first is the calculation of fully blanketed model atmospheres, in which account is taken of all sources of ultraviolet line and continuous opacity likely to be relevant to the Ap stars, with assumed elemental abundances of the sort deduced from ground-based spectra. It would be of great interest to see if abundance effects in the opacities were sufficient in themselves to explain the observed

ultraviolet flux deficiencies of the blue Ap stars. Secondly, the possible influence of strong magnetic fields on the atmospheric temperature-pressure structure and on the radiation field at a given point must be taken into account. An extended outer atmosphere, maintained by the stellar magnetic field, could be a potent source of ultraviolet opacity, if the thousands of lines of metallic ions and rare earths present shortward of  $3000\text{\AA}$  were enhanced in such a region by non-LTE effects or by magnetic desaturation.

The author is indebted to A. D. Code of the University of Wisconsin for the opportunity to use the Wisconsin Experiment Package on OAO-2 and data obtained therefrom. The assistance of A. V. Holm of the University of Wisconsin, J. J. Caldwell of Princeton University and S. R. Heap, W. M. Sparks and D. K. West of the Goddard Space Flight Center is gratefully acknowledged. Thanks must also be extended to J. F. McNall of the University of Wisconsin and to M. R. Molnar of LASP for valuable comments and discussion.

TABLE 1

## PECULIAR STARS OBSERVED

HD	Name or HR	Spectral Peculiarity	Pec. Source*	V	B-V	U-B	UBV Source*	Remarks†
358	$\alpha$ And	Hg, Mn	a, b	2.06	-0.11	-0.47	e	SB1, VB(9.2)
10783	...	Cr, Sr	a	6.56	-0.06	-0.16	g	
25267	$\tau^9$ Eri	Si3955	a	4.66	-0.14	-0.41	e	SB1
32650	1643	Si3955, Eu	a, b	5.44	-0.12	-0.36	f	
33904	$\mu$ Lep	Hg, Mn	a, b	3.29	-0.11	-0.39	e	
34452	1732	Si4200	a, b	5.35	-0.19	-0.62	f	
39317	137 Tau	Si, Cr	a, b	5.55	-0.06	-0.07	f	
40312	$\theta$ Aur	Si3955	a, b	2.62	-0.08	-0.18	e	VB(4.5)
68351	15 Cnc	Si3955, Cr	a, b	5.63	-0.08	-0.12	g	SB1
74521	49 Cnc	Si3955, Cr, Eu $\ddagger$	a, b	5.65	-0.10	-0.24	g	
78316	$\kappa$ Cnc	Hg	a	5.23	-0.11	-0.44	g	SB1
89822	4072	Hg, Mn $\S$	a, c, d	4.99	-0.07	-0.15	e	SB2
112413	$\alpha^2$ CVn	Si, Hg, Eu, Cr	a, b	2.89	-0.12	-0.32	e	VB(2.7)
120198	84 UMa	Eu, Cr	a, b	5.66	-0.05	-0.15	f	
133029	5597	Si3955, Sr, Cr	a, b	6.37	-0.10	-0.26	f	VB(3.2)
143807	$\iota$ CrB	Hg	a, b	4.98	-0.07	-0.20	e	
144206	$\upsilon$ Her	Hg, Mn	a, b	4.76	-0.11	-0.32	e	
149822	6176	Si, Cr, Sr	a, b	6.38	-0.08	-0.19	f	
173524	46 Dra	Hg, Mn	a, b, c	5.05	-0.12	-0.30	f	SB2
183056	4 Cyg	Si	a, b	5.16	-0.12	-0.41	f	SB1
184905	...	Si, Cr, Sr	a	6.43	-0.09	-0.27	f	
196178	7870	Si4200	a, b	5.77	-0.15	-0.54	f	
199728	20 Cap	Si4200	b	6.23	...	...	#	
223640	108 Aqr	Si4200, Sr, Cr	a, b	5.17	-0.16	-0.45	f	

-hc-

FOOTNOTES FOR TABLE 1

- \* a, Osawa (1965); b, Cowley et al. (1969); c, Conti (1970);  
d, Dworetzky (1972); e, Johnson et al. (1966); f, Eggen  
(1967); g, Stepien (1968b).
- + SB1, SB2 denote single or double-lined spectroscopic  
binaries (Abt and Snowden 1972). VB( $\Delta m$ ) denotes visual  
binaries with magnitude differences taken from Blanco  
et al. (1968) or Hoffleit (1964).
- ‡ Classified as Eu, Cr by Cowley et al. (1969).
- § Classified as Si, (Sr, Hg) by Cowley et al. (1969).
- || Corrected for interstellar extinction,  $E(B-V) = 0.06$ .
- # V from Hoffleit (1964).  $U-V \approx -0.53$  estimated from  
 $-2.5 \log F(4250\text{\AA})$  vs.  $U-V$  relation for unreddened Si  
stars.

TABLE 2  
NORMAL STARS OBSERVED

HD	Name or HR	MK Spectral Class	MK Class Source*	V	B-V	U-B	UBV Source*	Remarks†
14055	γ Tri	A1 V	b	4.01	+0.02	+0.02	d	
15008	δ Hyi	A2 V	a	4.09	+0.03	+0.05	d	
16978	ε Hyi	B9 III-V	a	4.11	-0.06	-0.14	d	
17081	π Cet	B7 V	a	4.25	-0.14	-0.45	d	
22928	δ Per	B5 III	a	2.92	-0.15	-0.53	d‡	SB1
23227	δ For	B5 IV	c	5.00	-0.16	-0.60	d	
24626	1214	B6 V	c	5.11	-0.13	(-0.52)	d§	
32630	η Aur	B3 V	a	3.18	-0.18	-0.67	d	
33802	ι Lep	B8 V	a	4.44	-0.09	-0.40	d	VB(6.3)
33949	κ Lep	B8 III-V	a	4.36	-0.10	-0.34	d	VB(2.9)
34759	ρ Aur	B5 V	a	5.22	-0.15	-0.58	e	SB1
37795	α Col	B8 Ve	a	2.64	-0.12	-0.46	d	VB(8.7)
38899	134 Tau	B9.5 V	b	4.91	-0.07	-0.16	d	
39844	ε Dor	B6 V	c	5.11	-0.14	-0.49	d	
41692	2154	B5 IV	a	5.29	-0.16	-0.56	d‡	VB(6.2)
45796	2360	B6 V	c	6.26	-0.13	(-0.48)	d§	
47105	γ Gem	A1 IV	b	1.92	0.00	+0.05	d	SB1
58715	β CMi	B8 V	a	2.89	-0.09	-0.27	d	
70011	λ Cnc	B9.5 V	b	5.91	-0.03	-0.12	e	
74198	γ Cnc	A1 IV	b	4.66	+0.02	+0.01	d	SB1
74280	η Hya	B3 V	a	4.30	-0.20	-0.74	d	SB1
82621	26 UMa	A2 V	b	4.51	0.00	+0.04	d	
95418	β UMa	A1 V	b	2.37	-0.02	0.00	d	
103287	γ UMa	A0 V	b	2.44	0.00	+0.03	d	SB1
106591	δ UMa	A3 V	b	3.31	+0.08	+0.07	d	
123299	α Dra	A0 III	b	3.65	-0.05	-0.08	d	SB1
147394	τ Her	B5 IV	a	3.90	-0.15	-0.56	d	VB(10.7)
160762	ι Her	B3 V	a	3.80	-0.18	-0.69	d	SB1
161868	γ Oph	A0 V	b	3.75	+0.04	+0.04	d	
186882	δ Cyg	B9.5 III	b	2.87	-0.02	-0.10	d	VB(4.9) SB1
193432	ν Cap	B9.5 V	b	4.76	-0.04	-0.11	d	VB(7.0)
201908	77 Dra	B8 V	b	5.92	-0.08	-0.24	f	
222173	ι And	B8 V	a	4.29	-0.11	-0.29	d	SB1

FOOTNOTES FOR TABLE 2

- \* a, Jaschek et al. (1964); b, Cowley et al. (1969); c, Hiltner et al. (1969); d, Johnson et al. (1966); e, Blanco et al. (1968); f, Stepien (1968a).
- † Notation and visual binary data sources same as for Table 1. Spectroscopic binary data from Hoffleit (1964), Jaschek et al. (1964) or Batten (1967).
- ‡ Corrected for interstellar extinction,  $E(B-V) = 0.03$ .
- § U-B estimated from  $-2.5 \log F(4250\text{\AA})$  vs. U-B relation for normal unreddened stars.

TABLE 3  
WEP FILTER CHARACTERISTICS

Photometer (S) Filter (F)	$\lambda$ (Å)*	$\delta\lambda$ (Å)†	$-2.5 \log \Delta$ ‡
S1 F3	4250	860	+1.705
S1 F1	3320	520	0.000
S1 F4	2980	410	-0.310
S3 F2	2460	360	-2.039
S3 F1	1910	260	-4.101
S4 F1	1550	270	-5.285
S4 F3	1430	240	-5.540

\* Effective wavelength for constant energy source.

† Bandwidth at 0.5 maximum sensitivity.

‡ Preliminary relative absolute calibration factors (Code 1971).

TABLE 4

APPARENT MAGNITUDES WITH THEIR UNCERTAINTIES AND NORMALIZED ABSOLUTE FLUX DISTRIBUTIONS\*

Name or HD	Effective Wavelength						Name or HD	Effective Wavelength							
	4250 $\text{\AA}$	3320 $\text{\AA}$	2980 $\text{\AA}$	2460 $\text{\AA}$	1910 $\text{\AA}$	1550 $\text{\AA}$		1430 $\text{\AA}$	4250 $\text{\AA}$	3320 $\text{\AA}$	2980 $\text{\AA}$	2460 $\text{\AA}$	1910 $\text{\AA}$	1550 $\text{\AA}$	1430 $\text{\AA}$
$\alpha$ And	...	-4.80	-4.67	...	-1.71	-0.97	-0.56	34452	-3.39	-1.84	-1.74	-0.26	+1.27	+2.35	+3.00
	...	0.04	0.04	...	0.02	0.04	0.07		0.02	0.02	0.02	0.02	0.02	0.07	0.09
	...	0.00	-0.18	...	-1.01	-1.46	-1.30		+0.16	0.00	-0.21	-0.46	-0.99	-1.10	-0.70
10783	-2.03	+0.17	+0.42	+2.07	+3.67	+5.04	+5.54	$\rho$ Aur	-3.48	-1.94	-1.94	-0.69	+0.67	+1.36	+1.62
	0.02	0.02	0.02	0.02	0.02	0.04	0.06		0.02	0.02	0.02	-0.02	0.02	0.04	0.04
	-0.50	0.00	-0.06	-0.14	-0.60	-0.42	-0.17		+0.17	0.00	-0.31	-0.79	-1.49	-1.99	-1.98
$\delta$ Hyi	-4.39	-1.93	-1.66	-0.01	+1.58	+3.14	+4.15	$\alpha$ Col	...	-4.18	-4.12	-2.78	-1.30	-0.57	-0.29
	0.04	0.02	0.02	0.02	0.02	0.05	0.05		...	0.04	0.04	0.04	0.02	0.05	0.03
	-0.76	0.00	-0.04	-0.12	-0.59	-0.22	+0.54		-0.05 $\ddagger$	0.00	-0.25	-0.64	-1.22	-1.68	-1.65
$\epsilon$ Hyi	-4.48	-2.33	-2.20	-0.76	+0.67	+1.52	+2.05	134 Tau	-3.72	-1.55	-1.43	-0.02	+1.41	+2.26	+2.77
	0.04	0.02	0.02	0.02	0.02	0.03	0.06		0.02	0.02	0.02	0.02	0.02	0.04	0.09
	-0.45	0.00	-0.18	-0.47	-1.10	-1.44	-1.16		-0.47	0.00	-0.19	-0.51	-1.14	-1.48	-1.22
$\eta$ Cet	-4.40	-2.66	-2.60	-1.25	+0.15	+0.90	+1.20	137 Tau	-3.01	-0.65	-0.37	+1.21	+2.74	+4.08	+4.63
	0.04	0.02	0.02	0.02	0.02	0.04	0.05		0.02	0.02	0.02	0.02	0.02	0.04	0.09
	-0.04	0.00	-0.25	-0.63	-1.29	-1.73	-1.68		-0.66	0.00	-0.03	-0.18	-0.71	-0.56	-0.26
$\delta$ Per $\dagger$	...	-3.96	-3.90	-2.50	-1.10	-0.39	-0.21	$\epsilon$ Dor	-3.61	-1.90	-1.87	-0.52	+0.91	+1.69	+1.94
	...	0.04	0.04	0.04	0.02	0.04	0.05		0.02	0.02	0.02	0.02	0.02	0.04	0.05
	+0.09 $\ddagger$	0.00	-0.26	-0.65	-1.34	-1.79	-1.87		-0.01	0.00	-0.28	-0.66	-1.29	-1.70	-1.70
$\delta$ For	-3.73	-2.18	-2.19	-0.92	+0.49	+1.22	+1.38	$\theta$ Aur	...	-3.73	-3.50	-1.89	-0.39	+1.07	+1.76
	0.02	0.02	0.02	0.03	0.02	0.03	0.06		...	0.02	0.02	0.02	0.02	0.04	0.05
	+0.16	0.00	-0.32	-0.78	-1.43	-1.89	-1.98		...	0.00	-0.08	-0.20	-0.76	-0.49	-0.05
24626	-3.61	-1.95	-1.95	-0.64	+0.75	+1.46	+1.66	41692 $\dagger$	-3.34	-1.70	-1.66	-0.33	+1.11	+1.85	+2.16
	0.02	0.02	0.02	0.02	0.02	0.04	0.09		0.02	0.02	0.02	0.02	0.02	0.04	0.09
	+0.05	0.00	-0.31	-0.73	-1.40	-1.88	-1.93		+0.08	0.00	-0.29	-0.75	-1.39	-1.82	-1.77
$\tau^9$ Eri	-4.00	-2.25	-2.07	-0.55	+0.92	+2.00	+2.60	45796	-2.46	-0.75	-0.70	+0.62	+2.06	+2.84	+3.09
	0.04	0.02	0.02	0.02	0.02	0.05	0.05		0.02	0.02	0.02	0.02	0.02	0.04	0.13
	-0.05	0.00	-0.13	-0.34	-0.93	-1.04	-0.69		-0.01	0.00	-0.26	-0.67	-1.29	-1.70	-1.70
$\eta$ Aur	...	-4.10	-4.14	-2.93	-1.59	-1.01	-0.78	$\gamma$ Gem	...	-4.03	-3.77	-2.06	-0.56	+0.86	+1.65
	...	0.04	0.04	0.04	0.02	0.04	0.04		...	0.04	0.04	0.02	0.02	0.03	0.04
	+0.28 $\ddagger$	0.00	-0.35	-0.87	-1.59	-2.20	-2.22		-0.74 $\ddagger$	0.00	-0.05	-0.07	-0.63	-0.40	+0.14
32650	-3.23	-1.29	-1.17	+0.25	+1.71	+2.74	+3.33	$\beta$ CMi	...	-3.72	-3.63	-2.17	-0.73	+0.07	+0.34
	0.02	0.02	0.02	0.02	0.02	0.04	0.09		...	0.02	0.02	0.02	0.02	0.05	0.04
	-0.24	0.00	-0.19	-0.50	-1.10	-1.26	-0.92		-0.29 $\ddagger$	0.00	-0.22	-0.49	-1.11	-1.50	-1.48
$\iota$ Lep	-4.20	-2.40	-2.34	-0.98	+0.42	+1.20	+1.51	15 Cnc	-3.03	-0.71	-0.44	+1.22	+2.72	+4.29	+4.83
	0.04	0.02	0.02	0.02	0.02	0.03	0.03		0.02	0.02	0.02	0.02	0.02	0.04	0.09
	-0.10	0.00	-0.25	-0.62	-1.28	-1.69	-1.63		-0.62	0.00	-0.04	-0.11	-0.67	-0.29	0.00
$\mu$ Lep	...	-3.50	-3.37	-1.93	-0.53	+0.31	+0.78	$\lambda$ Cnc	-2.66	-0.39	-0.22	+1.23	+2.74	+3.70	+4.23
	...	0.02	0.02	0.02	0.02	0.04	0.11		0.05	0.02	0.02	0.02	0.02	0.03	0.03
	...	0.00	-0.18	-0.47	-1.13	-1.48	-1.26		-0.57	0.00	-0.14	-0.42	-0.97	-1.20	-0.92
$\kappa$ Lep	-4.27	-2.38	-2.29	-0.88	+0.55	+1.34	+1.71	$\gamma$ Cnc	-3.83	-1.41	-1.15	+0.52	+2.06	+3.61	+4.33
	0.04	0.02	0.02	0.02	0.02	0.05	0.03		0.05	0.04	0.03	0.02	0.02	0.04	0.06
	-0.19	0.00	-0.22	-0.54	-1.17	-1.57	-1.45		-0.72	0.00	-0.05	-0.11	-0.63	-0.27	+0.20

-62-

TABLE 4 (continued)

Name or HD	Effective Wavelength							Name or HD	Effective Wavelength						
	4250Å	3320Å	2980Å	2460Å	1910Å	1550Å	1430Å		4250Å	3320Å	2980Å	2460Å	1910Å	1550Å	1430Å
η Hya	-4.43	-3.12	-3.17	-1.99	-0.66	+0.04	+0.20	τ Her	-4.81	-3.20	-3.20	-1.89	-0.54	+0.15	+0.35
	0.04	0.02	0.02	0.02	0.02	0.04	0.05		0.04	0.02	0.02	0.03	0.03	0.04	0.04
	+0.40	0.00	-0.36	-0.91	-1.64	-2.13	-2.22		+0.10	0.00	-0.31	-0.73	-1.44	-1.94	-1.99
49 Cnc	-3.01	-0.92	-0.67	+1.04	+2.59	+4.19	+4.70	149822	-2.29	-0.08	+0.29	+2.06	+3.64	+5.23	+5.81
	0.02	0.02	0.02	0.02	0.02	0.04	0.09		0.02	0.02	0.02	0.02	0.02	0.17	0.28
	-0.39	0.00	-0.06	-0.08	-0.59	-0.18	+0.08		-0.51	0.00	+0.06	+0.10	-0.38	+0.03	+0.35
x Cnc	-3.38	-1.65	-1.52	-0.10	+1.38	+2.35	+2.76	† Her	-4.94	-3.53	-3.57	-2.28	-0.98	-0.35	-0.20
	0.02	0.02	0.02	0.02	0.02	0.03	0.03		0.04	0.02	0.02	0.05	0.02	0.04	0.04
	-0.03	0.00	-0.18	-0.49	-1.07	-1.29	-1.13		+0.30	0.00	-0.35	-0.79	-1.55	-2.11	-2.21
26 UMa	-4.02	-1.53	-1.26	+0.41	+1.98	+3.37	+4.17	γ Oph	-4.77	-2.31	-2.10	-0.50	+1.12	+2.35	+3.10
	0.04	0.02	0.02	0.02	0.02	0.04	0.03		0.04	0.02	0.02	0.02	0.02	0.04	0.12
	-0.79	0.00	-0.04	-0.10	-0.59	-0.39	+0.16		-0.76	0.00	-0.10	-0.23	-0.67	-0.63	-0.13
89822	-3.65	-1.42	-1.22	+0.31	+1.81	+2.91	+3.42	46 Dra	-3.64	-1.57	-1.43	+0.02	+1.48	+2.50	+2.94
	0.02	0.02	0.02	0.02	0.02	0.07	0.09		0.02	0.02	0.02	0.02	0.02	0.04	0.09
	-0.53	0.00	-0.11	-0.31	-0.87	-0.96	-0.70		-0.37	0.00	-0.17	-0.45	-1.05	-1.22	-1.03
β UMa	...	-3.73	-3.50	-1.83	-0.34	+0.96	+1.75	4 Cyg	-3.52	-1.69	-1.59	-0.15	+1.32	+2.27	+2.73
	...	0.03	0.02	0.02	0.02	0.14	0.10		0.02	0.02	0.02	0.02	0.02	0.04	0.11
	-0.68±	0.00	-0.08	-0.14	-0.71	-0.60	-0.06		-0.13	0.00	-0.21	-0.50	-1.09	-1.33	-1.12
γ UMa	...	-3.62	-3.39	-1.76	-0.25	+1.04	+1.78	184905†	-1.96	+0.16	+0.40	+2.06	+3.56	+4.75	+5.19
	...	0.02	0.03	0.02	0.02	0.03	0.06		0.02	0.02	0.02	0.02	0.02	0.04	0.07
	-0.73±	0.00	-0.08	-0.18	-0.73	-0.63	-0.14		-0.37	0.00	-0.09	-0.28	-0.88	-0.85	-0.68
δ UMa	-5.14	-2.65	-2.34	-0.59	+1.02	+3.08	+4.22	δ Cyg	...	-3.34	-3.14	-1.57	-0.09	+0.95	+1.45
	0.04	0.02	0.02	0.02	0.02	0.03	0.03		...	0.02	0.02	0.02	0.02	0.03	0.03
	-0.79	0.00	0.00	+0.02	-0.43	+0.45	+1.33		-0.61±	0.00	-0.11	-0.27	-0.85	-1.00	-0.75
α <sup>2</sup> CVn§	...	-3.81	-3.62	-1.93	-0.43	+0.77	+1.39	ν Cap	-3.82	-1.53	-1.37	+0.12	+1.60	+2.58	+3.19
	...	0.02	0.02	0.02	0.02	0.04	0.06		0.02	0.02	0.02	0.02	0.02	0.04	0.06
	...	0.00	-0.12	-0.16	-0.72	-0.71	-0.34		-0.59	0.00	-0.15	-0.39	-0.97	-1.18	-0.82
84 UMa	-2.92	-0.87	-0.33	+1.29	+2.83	+4.28	+4.97	196178	-2.97	-1.31	-1.24	+0.17	+1.65	+2.65	+3.08
	0.02	0.02	0.02	0.02	0.02	0.04	0.10		0.02	0.02	0.02	0.02	0.02	0.04	0.11
	-0.55	0.00	+0.03	-0.08	-0.60	-0.34	+0.10		+0.05	0.00	-0.24	-0.56	-1.14	-1.33	-1.15
α Dra	-4.93	-2.56	-2.38	-0.83	+0.66	+1.72	+2.25	20 Cap	-2.42	-0.59	-0.46	+1.04	+2.53	+3.73	...
	0.04	0.02	0.02	0.02	0.02	0.04	0.05		0.02	0.02	0.02	0.02	0.02	0.08	...
	-0.67	0.00	-0.13	-0.31	-0.88	-1.01	-0.73		-0.13	0.00	-0.18	-0.41	-0.98	-0.97	...
133029	-2.37	-0.29	-0.05	+1.63	+3.16	+4.58	+5.07	77 Dra	-2.72	-0.67	-0.57	+0.81	+2.26	+3.13	...
	0.02	0.02	0.02	0.02	0.02	0.04	0.05		0.03	0.02	0.02	0.02	0.02	0.04	...
	-0.38	0.00	-0.07	-0.12	-0.65	-0.42	-0.18		-0.35	0.00	-0.21	-0.56	-1.17	-1.49	...
† CrB	-3.63	-1.46	-1.29	+0.21	+1.70	+2.73	+3.19	108 Aqr	-3.48	-1.71	-1.59	-0.10	+1.42	+2.40	+2.93
	0.02	0.02	0.02	0.02	0.02	0.07	0.06		0.02	0.02	0.02	0.02	0.02	0.04	0.09
	-0.47	0.00	-0.14	-0.37	-0.94	-1.10	-0.89		-0.07	0.00	-0.19	-0.43	-0.97	-1.18	-0.90
υ Her	-3.90	-1.95	-1.77	-0.37	+1.12	+1.99	+2.40								
	0.04	0.02	0.02	0.02	0.02	0.04	0.05								
	-0.25	0.00	-0.13	-0.46	-1.03	-1.35	-1.19								

\* For each star top row of data gives  $m'(\lambda)$ , second row gives uncertainty in  $m'(\lambda)$ , third row gives  $-2.5 \log F(\lambda)$ .

†  $-2.5 \log F(\lambda)$  values corrected for reddening with average extinction law of Bless and Savage (1972).

‡ Value estimated from  $-2.5 \log F(4250\text{Å})$  vs. (U-V) relation for normal, unreddened stars.

§ Data for phase 0.0 taken from Molnar (1972) and reduced to consistency with present photometric system.

TABLE 5

CLASSIFICATION OF Ap STARS ON THE BASIS OF THEIR  
ULTRAVIOLET FLUX DISTRIBUTIONS

Name or HD	UBV Comparison Stars*	UBV Class†	Ultraviolet Comparison Stars‡	Ultra- violet Class	MK Class	MK Class Source §
$\alpha$ And	$\alpha$ Col	B6-B7	134 Tau	B9	B9 p	a
10783	$\epsilon$ Hyi	B9	$\gamma$ Gem, 26 UMa	A1	A2 p	b
$\tau^9$ Eri	$\pi$ Cet	B6-B7	$\nu$ Cap, $\alpha$ Dra	B9.5	A0 p	b
32650	$\alpha$ Col, $\kappa$ Lep	B7-B8	$\epsilon$ Hyi, $\nu$ Cap	B9-B9.5	B9 p	a
$\mu$ Lep	$\alpha$ Col, $\kappa$ Lep	B7	134 Tau	B9	B9 p	a
34452	$\iota$ Her, $\delta$ For	B3-B5	134 Tau, $\nu$ Cap	B9.5	A0 p	a
137 Tau	$\delta$ Cyg, $\alpha$ Dra	B9-B9.5	$\gamma$ Oph	A0	B9 p	a
$\theta$ Aur	134 Tau	B8-B9	$\gamma$ UMa, $\gamma$ Gem	A0-A1	A0 p	a
15 Cnc	$\epsilon$ Hyi	B8-B9.5	$\gamma$ Oph, $\gamma$ Cnc	A1	B9 p	a
49 Cnc	$\beta$ CMi	B8	$\gamma$ Cnc, 26 UMa	A1-A2	A1 p	a
$\kappa$ Cnc	$\alpha$ Col	B7	$\epsilon$ Hyi	B9	B8 p	b
89822	134 Tau	B9	$\alpha$ Dra	B9.5-A0	A0 p	a
$\alpha^2$ CVn	$\kappa$ Lep	B7-B8	$\alpha$ Dra, $\gamma$ UMa	A0	A0 p	a
84 UMa	$\epsilon$ Hyi	B9	$\gamma$ Gem, 26 UMa	A1-A2	B9 p	a
133029	$\beta$ CMi	B8	$\gamma$ Oph, $\gamma$ Cnc	A1	B9 p	a
$\iota$ CrB	77 Dra, 134 Tau	B9	$\nu$ Cap, $\alpha$ Dra	B9.5	A0 p	a
$\upsilon$ Her	$\kappa$ Lep	B7-B8	134 Tau, $\lambda$ Cnc	B9-B9.5	B9 p	a
149822	77 Dra, 134 Tau	B8-B9	$\delta$ Hyi	later than A2	B9 p	a
46 Dra	$\kappa$ Lep	B7-B8	134 Tau, $\lambda$ Cnc	B9-B9.5	B9.5 p	a
4 Cyg	$\alpha$ Col	B7	$\epsilon$ Hyi	B9	B9 p	a
184905	$\beta$ CMi	B8	$\delta$ Cyg	B9.5-A0	A0 p	b
196178	$\tau$ Her	B5	77 Dra, $\epsilon$ Hyi	B8-B9	B9 p	a
20 Cap	$\iota$ Lep, $\pi$ Cet	B7	$\nu$ Cap, $\delta$ Cyg	B9.5	B9 p	a
108 Aqr	$\delta$ For, $\pi$ Cet	B5-B7	$\lambda$ Cnc	B9.5	B9 p	a

FOOTNOTES FOR TABLE 5

- \* Normal stars listed in Tables 2 and 4 with UBV colors similar to those of the Ap star in question.
- † Based on colors given in Table 1 and Johnson's (1963) standard sequence.
- ‡ Normal stars listed in Tables 2 and 4 with ultraviolet flux distributions closely resembling that of the Ap star in question.
- § a, Cowley et al. (1969); b, Jaschek et al. (1964).

## REFERENCES

- Abt, H. A. and Snowden, M. S. 1972, Ap. J. Suppl., in press.
- Adams, T. F. and Morton, D. C. 1968, Ap. J., 152, 195.
- Babcock, H. W. 1958, Ap. J., 128, 228.
- Batten, A. H. 1967, Pub. D.A.O., 13, 119.
- Bernacca, P. L. and Molnar, M. R. 1972, Ap. J., 178, 189.
- Bertaud, C. 1959, Journ. des Obs., 42, 45.
- Blanco, V. M., Demers, S., Douglass, G. G. and Fitzgerald, M. P. 1968, Pub. Naval Obs., 21, 1.
- Bless, R. C. and Savage, B. D. 1972, Ap. J., 171, 293.
- Code, A. D. 1969, Pub. A.S.P., 81, 475.
- Code, A. D. 1971, private communication.
- Code, A. D., Houck, T. E., McNall, J. F., Bless, R. C. and Lillie, C. F. 1970, Ap. J., 161, 377.
- Conti, P. S. 1970, Ap. J., 160, 1077.
- Cowley, A., Cowley, C., Jaschek, M. and Jaschek, C. 1969, A. J., 74, 375.
- Deutsch, A. J. 1947, Ap. J., 105, 283.
- Dieke, G. H., Crosswhite, H. M. and Dunn, B. 1961, J. Opt. Soc. America, 51, 820.
- Dworetzky, M. M. 1972, private communication.
- Eggen, O. J. 1967, in The Magnetic and Related Stars, ed. R. C. Cameron (Baltimore: Mono Book Corp.), P. 141.
- Hiltner, W. A., Garrison, R. F. and Schild, R. E. 1969, Ap. J., 157, 313.

- Hoffleit, D. 1964, Catalogue of Bright Stars, Yale University Observatory.
- Hyland, A. R. 1967, in The Magnetic and Related Stars, ed. R. C. Cameron (Baltimore: Mono Book Corp.), p. 311.
- Jaschek, C., Conde, H. and de Sierra, A. C. 1964, Catalogue of Stellar Spectra Classified in the Morgan-Keenan System, LaPlata Observatory.
- Johnson, H. L. 1963, in Basic Astronomical Data, ed. K. Aa. Strand (Chicago: University of Chicago Press), p. 204.
- Johnson, H. L., Mitchell, R. I., Iriarte, B. and Wisniewski, W. Z. 1966, Comm. Lunar and Planet. Lab., <sup>^</sup>4, 99.
- Jugaku, J. and Sargent, W. L. W. 1968, Ap. J., <sup>^</sup>151, 259.
- Klinglesmith, D. A. 1971, private communication.
- \_\_\_\_\_ 1972, ibid.
- Mihalas, D. and Henshaw, J. L. 1966, Ap. J., <sup>^</sup>144, 25.
- Molnar, M. R. 1973, Ap. J., in press.
- Osawa, K. 1959, Ap. J., <sup>^</sup>130, 159.
- \_\_\_\_\_ 1965, Annals Tokyo Astron. Obs., 2nd Ser., <sup>^</sup>9, 123.
- Peterson, D. M. 1970, Ap. J., <sup>^</sup>161, 685.
- Preston, G. W. 1970, in Stellar Rotation, ed. A. Slettebak (Dordrecht, Holland: D. Reidel Publishing Co.), p. 254.
- \_\_\_\_\_ 1971, Pub. A.S.P., <sup>^</sup>83, 571.
- Sargent, W. L. W. and Searle, L. 1967, in The Magnetic and Related Stars, ed. R. C. Cameron (Baltimore: Mono Book Corp.), p. 209.

Searle, L. and Sargent, W. L. W. 1964, Ap. J., <sup>~~~~</sup>139, 793.

Stepien, K. 1968a, Ap. J., <sup>~~~~</sup>153, 165.

\_\_\_\_\_ 1968b, ibid., <sup>~~~~</sup>154, 945.

Strom, S. E. and Strom, K. M. 1969, Ap. J., <sup>~~~~</sup>155, 17.

Underhill, A. B., Leckrone, D. S. and West, D. K. 1972,

Ap. J., <sup>~~~~</sup>171, 63.

Wolff, S. C. and Wolff, R. J. 1971, A. J., <sup>~~~~</sup>76, 422.

## LEGENDS FOR THE FIGURES

Fig. 1. - Normalized absolute fluxes in magnitude units at  $2460\text{\AA}$  and  $1910\text{\AA}$  plotted versus U-V for various classes of Ap stars and for comparison standard dwarfs and giants. Darkened circles, normal stars. Open circles, Si 3955,4200 stars. X's, other Si stars. Open squares, Hg-Mn stars. Open triangles, Sr-Cr-Eu stars. Ap stars are deficient in  $-2.5 \log F(\lambda)$  compared to normal stars of similar U-V. Hg-Mn stars appear less flux deficient, for their U-V colors, than do Si or Sr-Cr-Eu stars.

Fig. 2. - Normalized absolute fluxes in magnitude units at  $1550\text{\AA}$  and  $1430\text{\AA}$  plotted versus U-V for various classes of Ap stars and for comparison standard dwarfs and giants. Symbols and description same as for Figure 1.

Fig. 3. - Normalized absolute flux distributions of individual Ap stars compared to those of selected normal stars. Individual data points for Ap stars are denoted by X's. Data points for normal stars are connected by lines. Dashed lines represent normal stars with UBV colors similar to those of Ap star. Solid lines represent normal stars whose flux distributions at  $\lambda \leq 3320\text{\AA}$  most closely resemble that of Ap star. a. 108 Aqr, ordinate axis labeled at left. The ultraviolet flux distribution of 108 Aqr (B9p) closely resembles that of  $\lambda$  Cnc (B9.5), although 108 Aqr has UBV

colors like those of  $\pi$  Cet (B7) and  $\delta$  For (B5). b.  $\theta$  Aur, ordinate axis labeled at right.  $\theta$  Aur (A0p) resembles 134 Tau (B9) in its UBV colors but has an ultraviolet flux distribution similar to early A stars like  $\gamma$  UMa (A0).

Fig. 4. - Format and symbols same as in Figure 3.

a. HR 1732, ordinate axis labeled at left. HR 1732 (A0p) has an ultraviolet flux distribution similar to that of  $\nu$  Cap (B9.5), although its UBV colors resemble those of  $\iota$  Her (B3) and  $\delta$  For (B5). b. 49 Cnc, ordinate axis labeled at right. The ultraviolet flux distribution of 49 Cnc (A1p) is nearly identical to that of  $\gamma$  Cnc (A1), although 49 Cnc has UBV colors similar to those of  $\delta$  CMi (B8).

Fig. 5. - Format and symbols same as in Figure 3.

a.  $\tau^9$  Eri, ordinate axis labeled at left.  $\tau^9$  Eri (A0p) resembles  $\pi$  Cet (B7) in its UBV colors but possesses an ultraviolet flux distribution resembling those of  $\nu$  Cap (B9.5) and  $\alpha$  Dra (A0). b.  $\iota$  CrB, ordinate axis labeled at right. The ultraviolet flux distribution of  $\iota$  CrB (A0p) is similar to those of  $\nu$  Cap (B9.5) and  $\alpha$  Dra (A0), although  $\iota$  CrB has UBV colors like those of 77 Dra (B8).

Fig. 6. - Format and symbols same as in Figure 3.

a. 15 Cnc, ordinate axis labeled at left. 15 Cnc (B9p) has UBV colors similar to those of 134 Tau (B9) and  $\nu$  Cap (B9.5) but its ultraviolet flux distribution resembles those of

early A stars like  $\gamma$  Cnc (A1). The MK class of 15 Cnc listed in Table 5 would imply a non-existent UBV color-spectral class discrepancy for this Si Star (see discussion in §IV).

b. HD 10783, ordinate axis labeled at right. The ultraviolet flux distribution of HD 10783 (A2p) resembles those of early A stars like  $\gamma$  Gem (A1) or 26 UMa (A2), although it possesses UBV colors like those of  $\epsilon$  Hyi. (B9).

Fig. 7. - WEP Spectrometer 1 scans of  $\theta$  Aur, denoted by X's, and four normal comparison stars. Dotted lines connect data points for  $\iota$  And (B8), a star with UBV colors approximating those of  $\theta$  Aur (see discussion in §V). Data points for  $\delta$  Cyg (B9.5),  $\gamma$  Tri (A1) and  $\gamma$  Gem (A1) are connected by dashed lines, solid lines and solid lines with open circles, respectively. The  $20\text{\AA}$  bandpass data are normalized to zero magnitudes at  $3318\text{\AA}$ . Half-power bandpasses of three WEP filters are shown. At no point does  $\theta$  Aur approach in relative brightness a normal star of similar UBV colors, but it differs in detail from all normal stars shown.

Fig. 8. - WEP Spectrometer 2 scans of  $\theta$  Aur, denoted by X's, and three normal comparison stars. Dashed lines connect data points for  $\beta$  CMi, a star which differs insignificantly from  $\theta$  Aur in its UBV colors. Solid lines and dash-dot lines connect data points for  $\gamma$  UMa (A0) and  $\gamma$  Gem (A1), respectively. The  $10\text{\AA}$  bandpass data are normalized to  $U=0.00$  mag. The half-power

bandpass of the 1550 $\text{\AA}$  WEP filter is shown.  $\theta$  Aur data are bracketed by data for  $\gamma$  UMa and  $\gamma$  Gem both here and in comparable broad-band data in Figure 3b. At no point does  $\theta$  Aur approach in relative brightness a normal star of similar UBV colors.

FIGURE 1

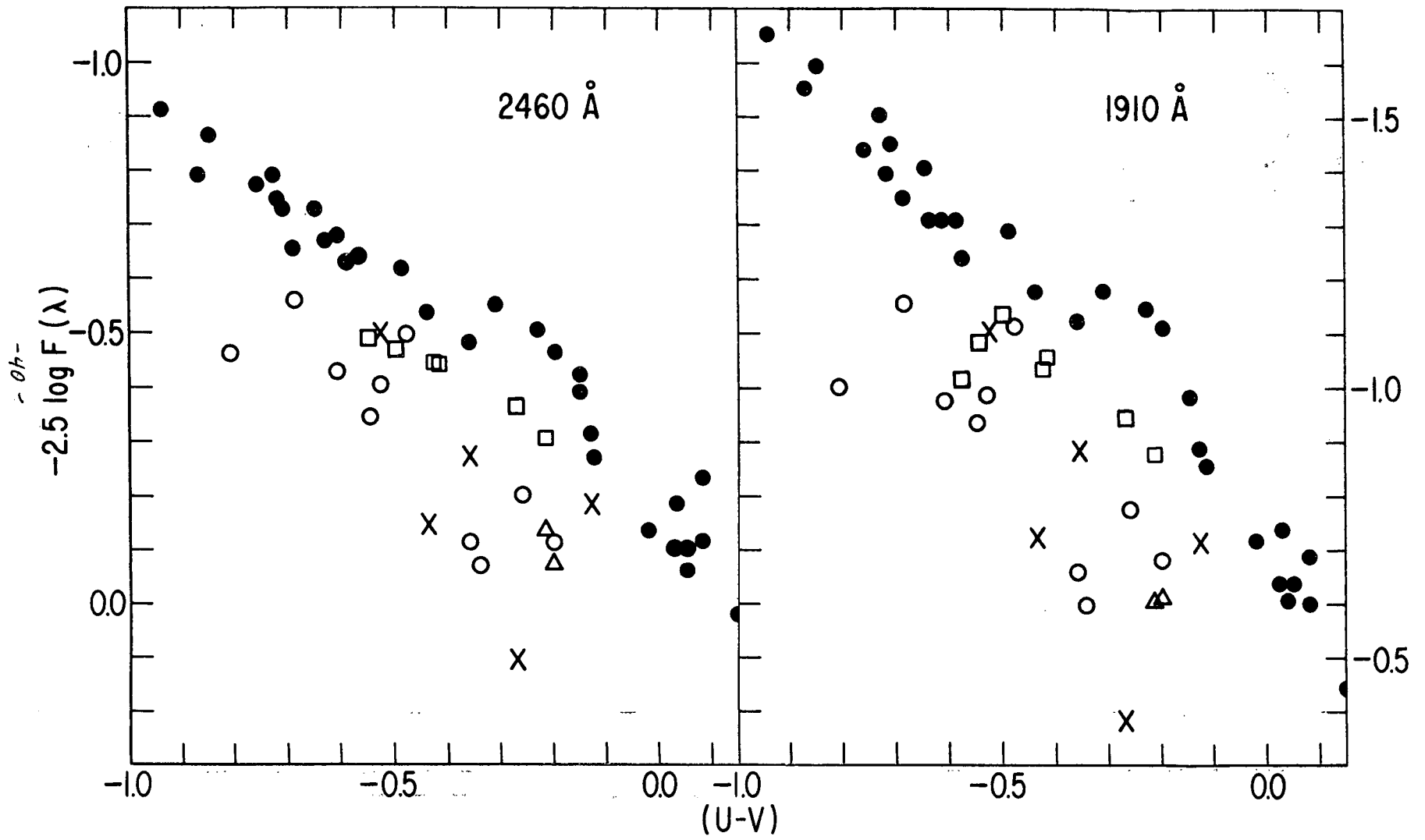


FIGURE 2

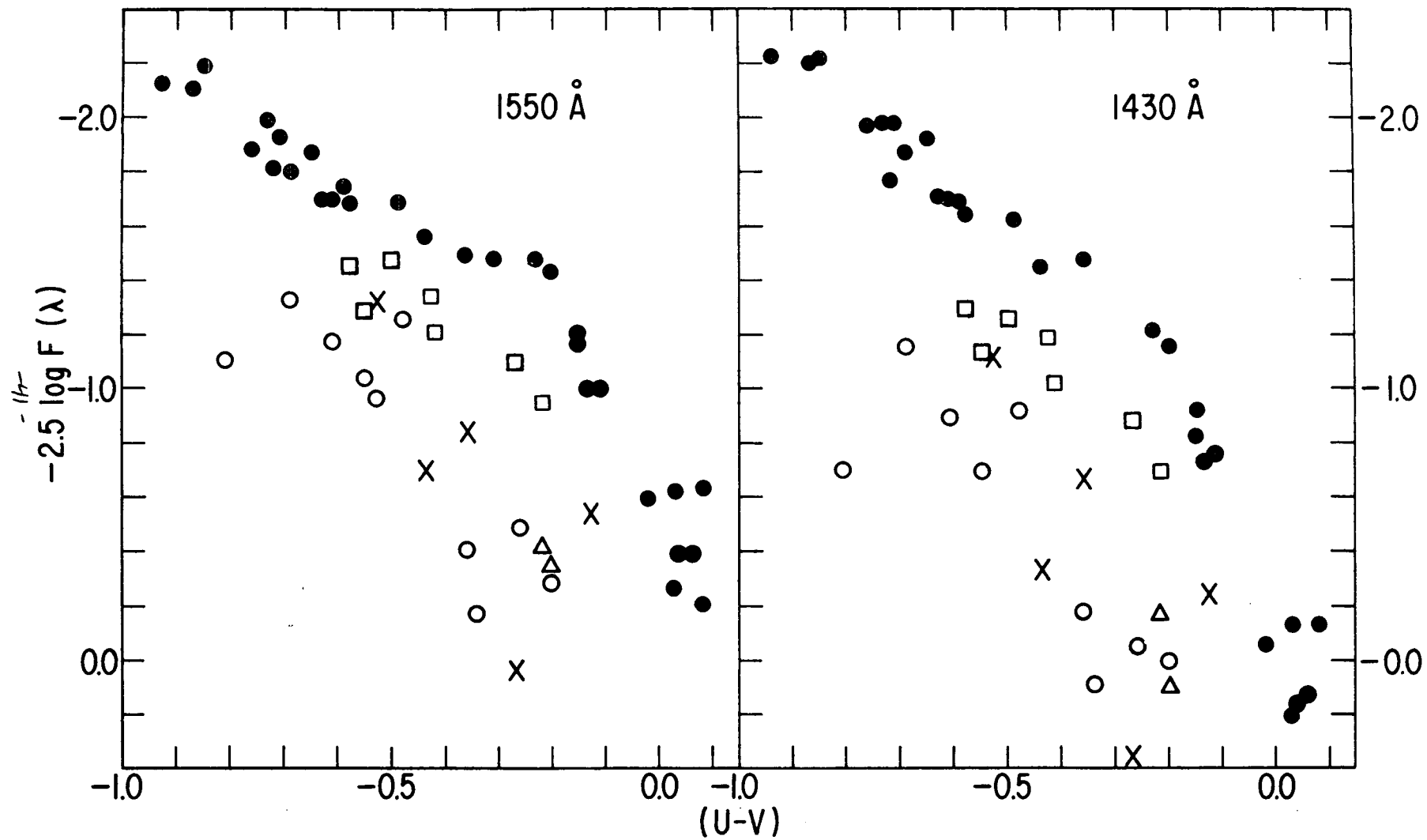


FIGURE 3

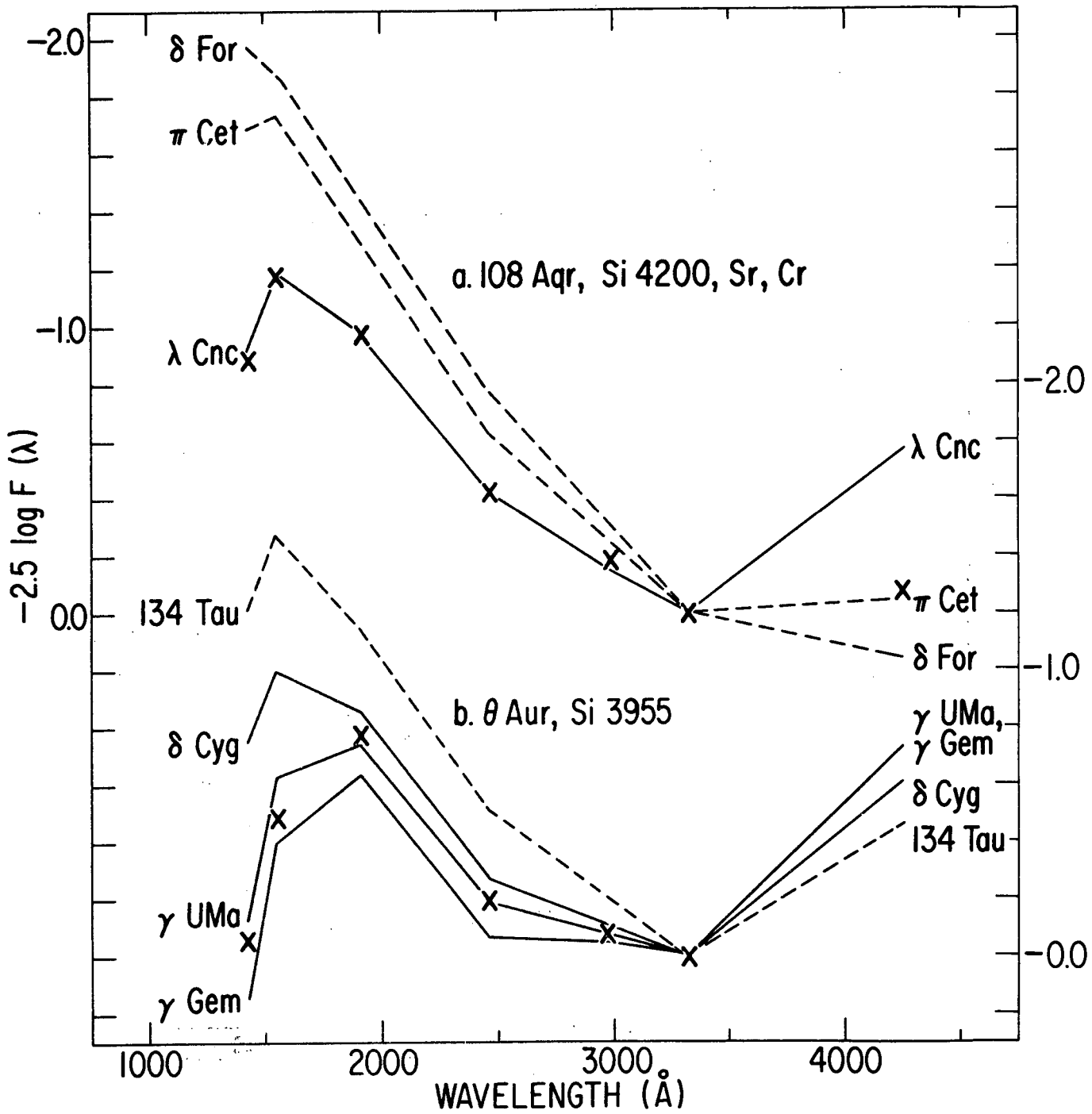


FIGURE 4

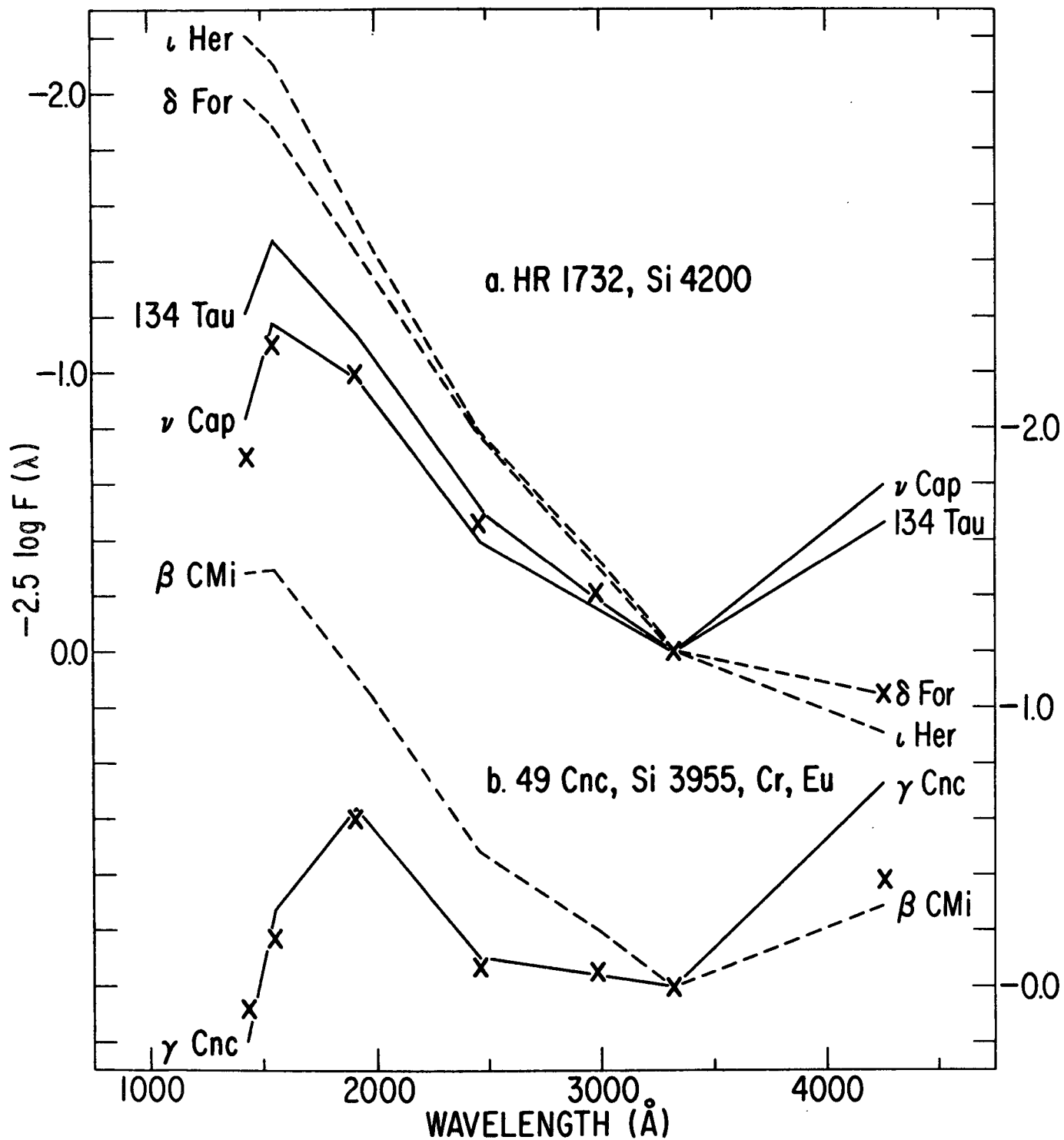


FIGURE 5

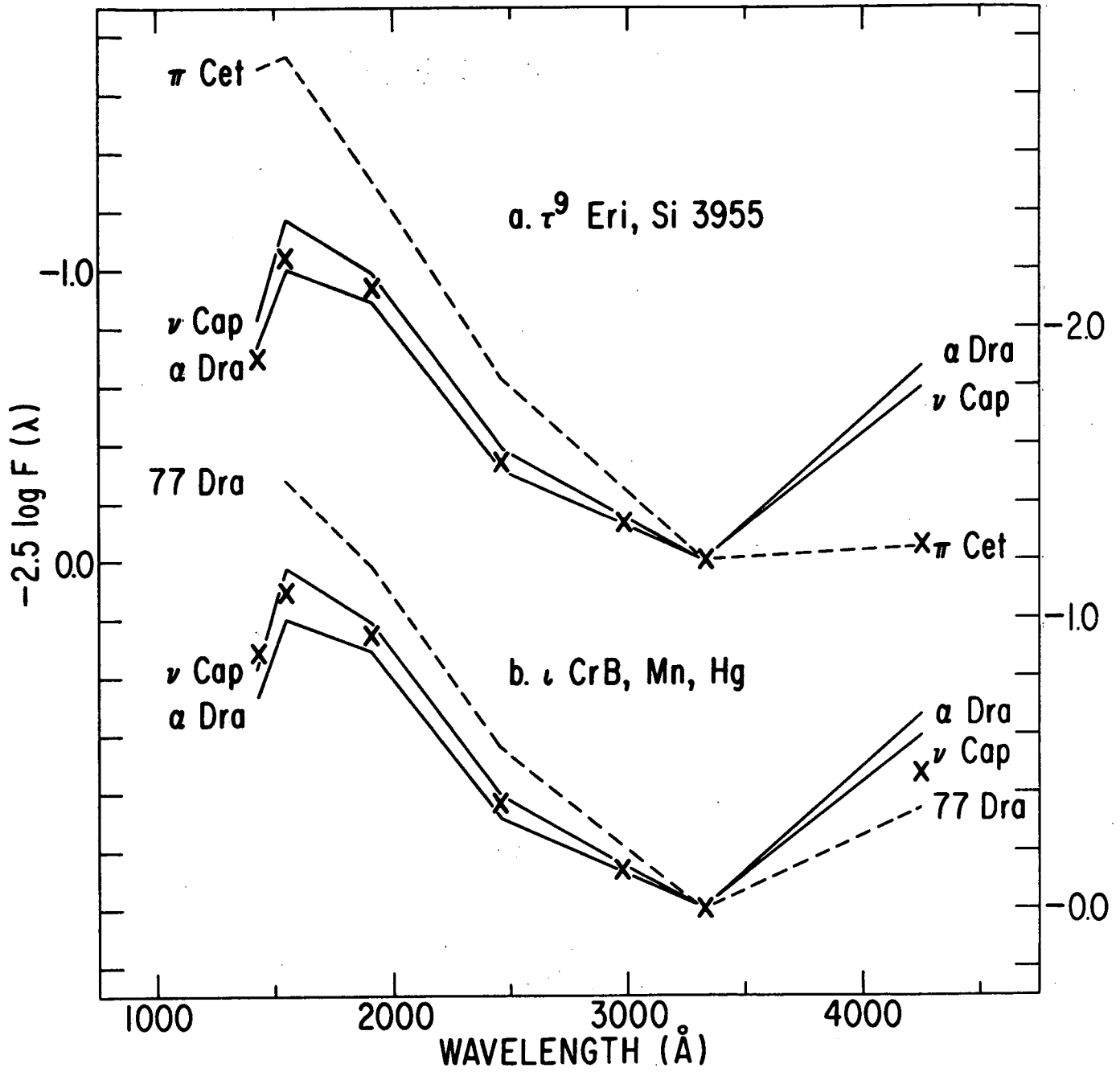


FIGURE 6

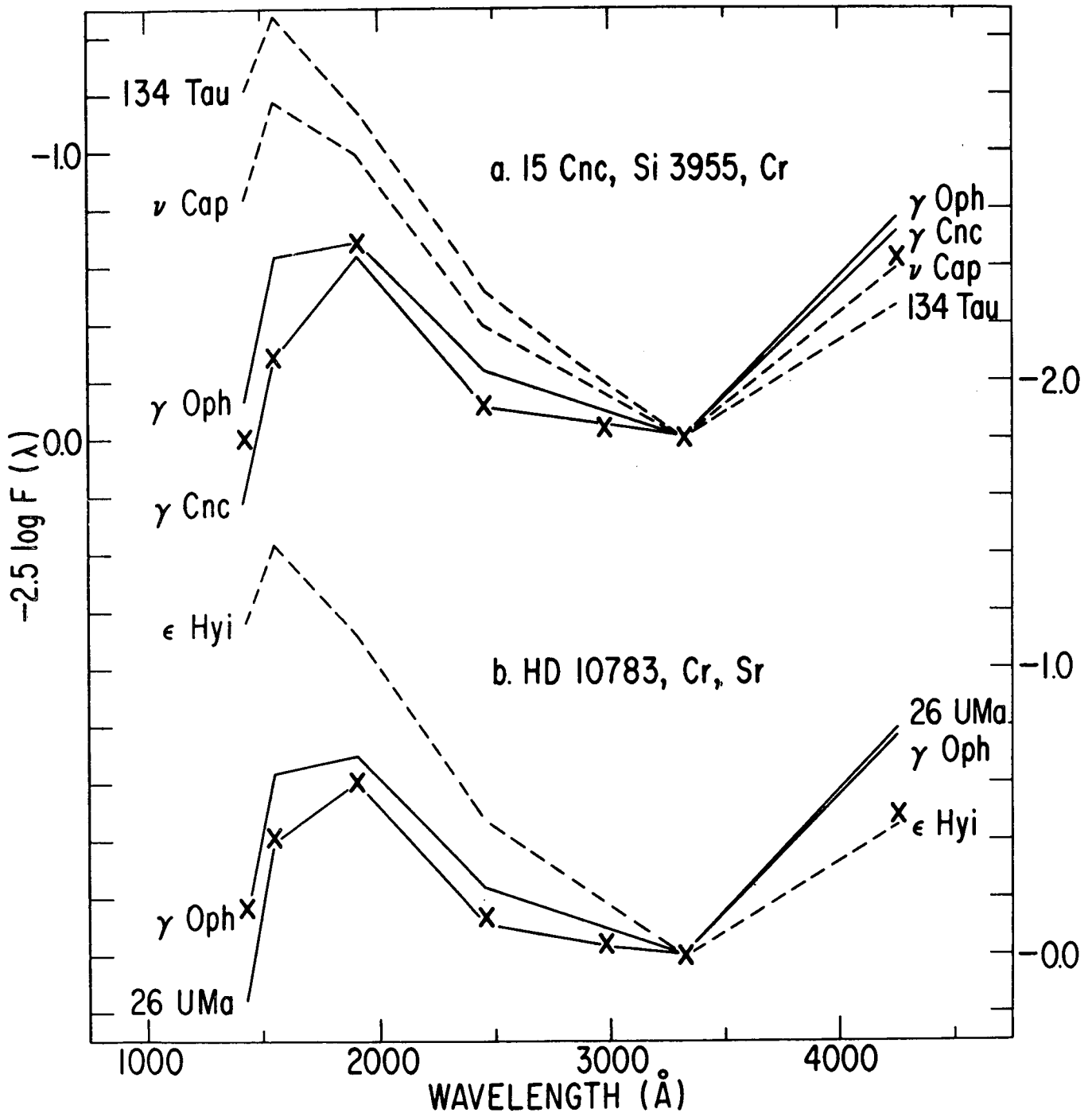


FIGURE 7

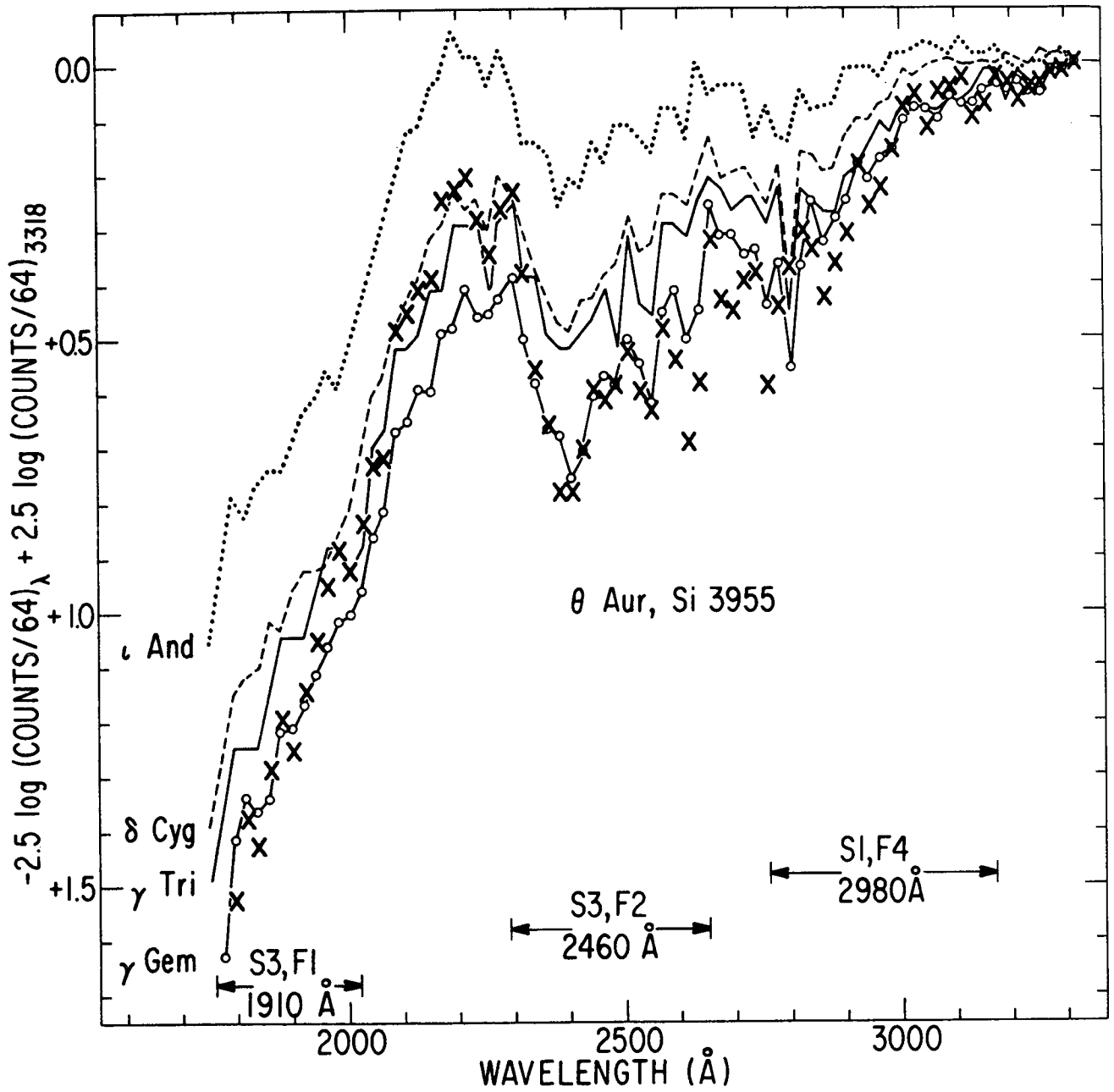


FIGURE 8

